

Solar Evaporation Enhancement Using Floating light-absorbing Magnetic Particles

Yao Zeng, Jianfeng Yao, Bahman Amini Horri, Kun Wang, Yuzhou Wu, Dan Li and Huanting
Wang*

Department of Chemical Engineering, Monash University, Clayton, Victoria 3800, Australia Tel:
+61 3 9905 3449; E-mail: huanting.wang@monash.edu

Supplementary Information

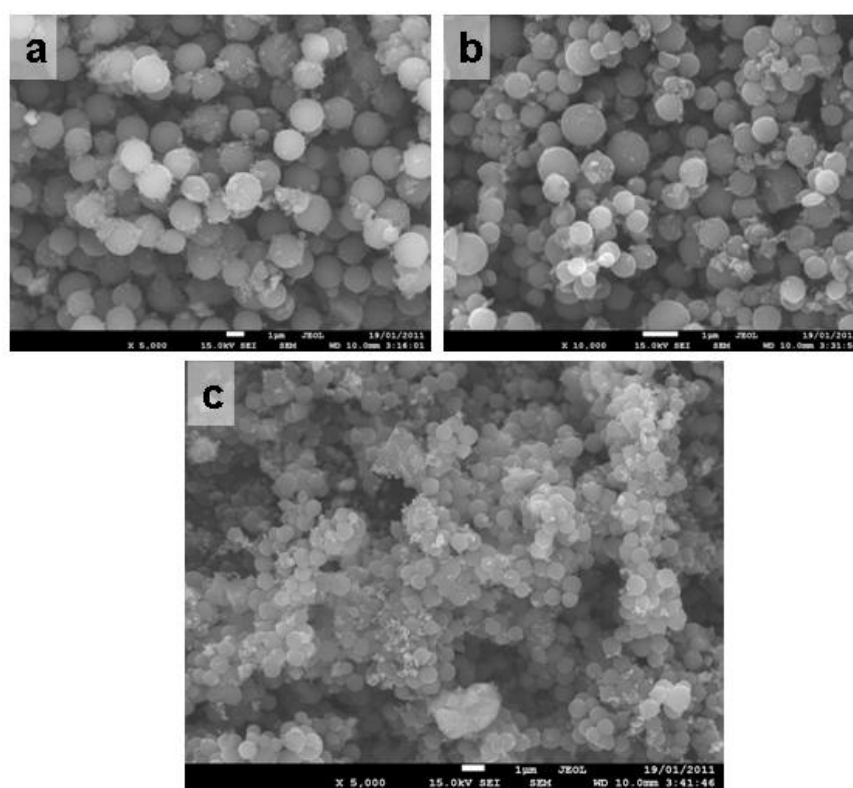


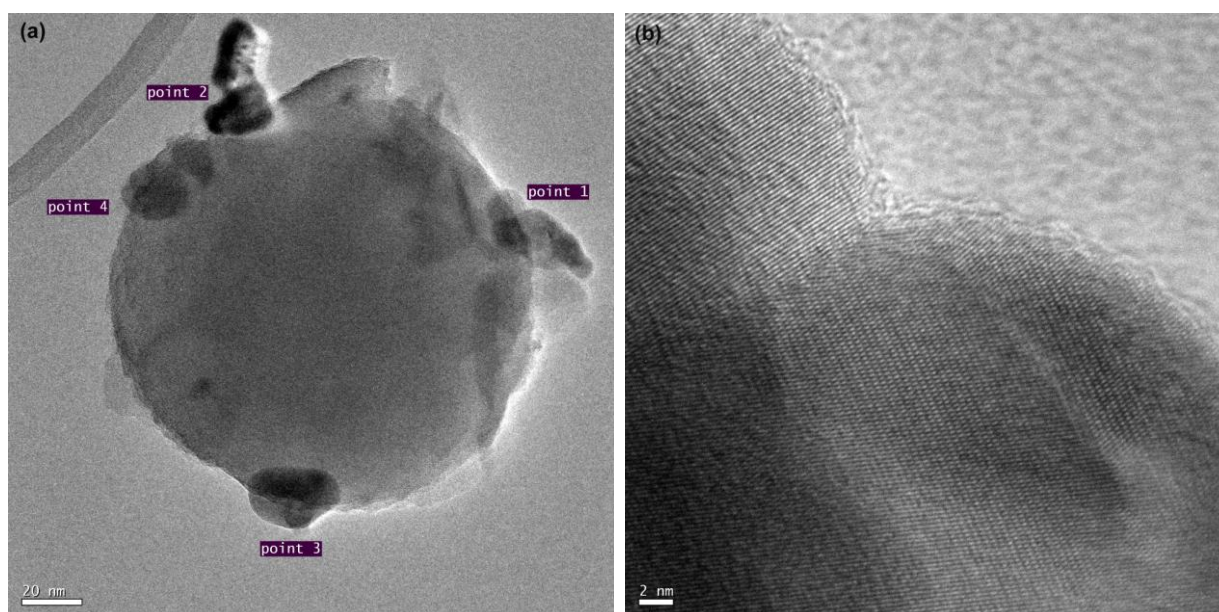
Fig. S1. SEM images of $\text{Fe}_3\text{O}_4/\text{C}$ particles prepared from 1 g of Fe_3O_4 , 10 g of F127, 6 g of water, x g of FA and 1.4 g of hydrochloric acid, and y mL of ethanol: (a) x = 6, y = 25, (b) x = 6, y = 35, and (c) x = 7, y = 30. The length of scale bar on all images is 1 μm . The SEM images reveal that these samples contain many small particles.

The density is 1.56 g cm^{-3} for sample (a), 1.62 g cm^{-3} for sample (b), and 1.65 g cm^{-3} for sample (c). The densities of these samples are slightly greater than the density of the sample shown in Fig.1. On

the basis of the morphologies and densities, the sample shown in Fig.1 was chosen for solar evaporation tests.



Fig. S2. Photos showing that Fe₃O₄/C particles are fully dispersed in water after addition of a small amount of polyvinylpyrrolidone as a dispersant (left), and the majority of Fe₃O₄/C particles still float on water after stirring overnight, and boiling and ultrasonication for hours (right).



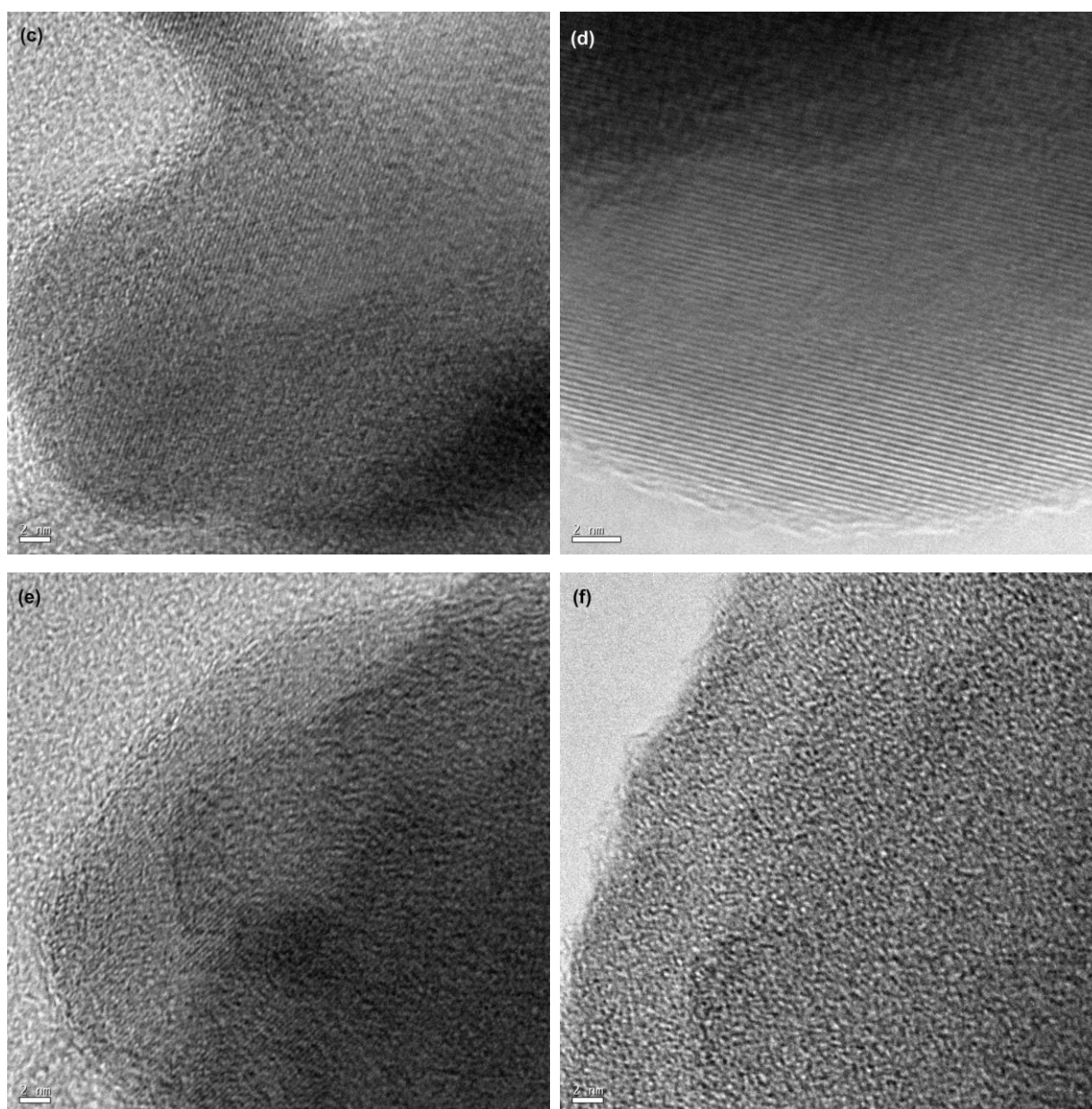


Fig. S3. (a) TEM image of a representative $\text{Fe}_3\text{O}_4/\text{C}$ particle, and (b-f) High-resolution TEM images of this particle in different areas: (b) point 1, (c) point 2, (d) point 3, (e) point 4, and (f) carbon edge. These images indicate that particles in points 1-4 are crystalline Fe_3O_4 , and the carbon is amorphous.

Mathematical Modeling

Governing Equation

The salt water evaporation process using the floating porous material (packed $\text{Fe}_3\text{O}_4/\text{C}$ particles) on the surface was modeled using the transient energy conservation over the solid and liquid phases.

The geometry of the physical system consists of the porous materials and salt water shown in Fig.

S4.

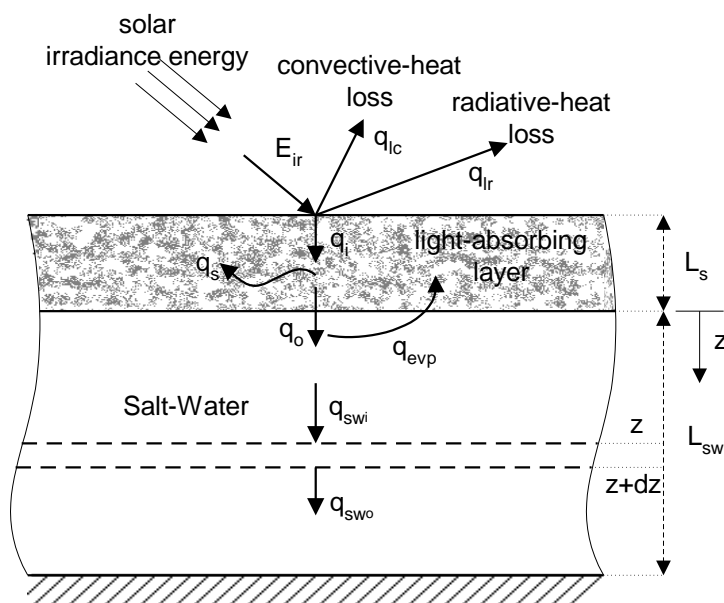


Fig. S4. Geometry of the analysed physical system

The solid phase was treated as the lumped geometry due to its very low Biot number ($Bi \leq 0.0083$) and it was also assumed that the heat conduction mechanism could prevail the heat transfer inside the salt water phase. It was assumed that the air condition (temperature, pressure, and relative humidity), the solar irradiance, and the liquid-phase level are constant during the evaporation process.

The governing equation for the solid material in the transient period depends on the values of the solid-phase and ambient temperatures (T_s and T_a) and can be written as:

$$E_{ir} + h_a(1 - \phi)(T_a - T_s) - N_w \cdot \Delta H_{fg} \cdot \phi - h_w(1 - \phi)(T_s - T_{sw}) - \rho_m \cdot C_{p_m} \cdot l_s \cdot \frac{dT_s}{d\theta} = 0 \quad (\text{if: } T_s \leq T_a) \quad (1)$$

$$E_{ir} - \delta(\epsilon \cdot T_s^4 - T_a^4) - h_a(1 - \phi)(T_a - T_s) - N_w \cdot \Delta H_{fg} \cdot \phi - h_{sw}(1 - \phi)(T_s - \bar{T}_{sw}) - \rho_m \cdot C_{p_m} \cdot l_s \cdot \frac{dT_s}{d\theta} = 0 \quad (\text{if: } T_s > T_a) \quad (2)$$

The first four terms in equation (1) represent the absorbed solar irradiance energy, the energy obtained by convection, the energy loss by evaporation, and the energy transferred into the liquid-phase. Equation (2) is valid at the solid temperature higher than the ambient temperature (T_a) and compared to equation (1), it has an additional term for the radiation heat loss from surface of the solid phase. The last term in both equations stands for the transient temperature differential change in the porous solid phase. The initial condition for equations (1) and (2) can be expressed as:

$$@ \theta = 0: T_s = T_{sw}^{sat} \quad (3)$$

This means the evaporation process starts at the uniform saturation temperature of salt water for both phases.

The governing equation for the salt water phase in the transient period and the domain of $0 \leq z \leq l_{sw}$ was derived as:

$$\alpha_{sw} \cdot \frac{\partial^2 T_{sw}}{\partial z^2} - \frac{\partial T_{sw}}{\partial \theta} = 0 \quad (4)$$

The first and second term in equation (4) represent the one dimensional conductive heat transfer term and the transient temperature differential change inside the liquid phase respectively. The initial and boundary conditions for equation (4) can be expressed as:

$$@ \theta = 0: T_{sw} = T_{sw}^{sat} \quad (5)$$

$$@ z = 0, any \theta > 0: -K_{sw} \frac{\partial T_{sw}}{\partial z} = h_{sw}(1 - \phi)(T_s - T_{sw}) \quad (6)$$

$$@ z = l_{sw}, any \theta > 0: \frac{\partial T_{sw}}{\partial z} = 0 \quad (7)$$

Equations (5) to (6) represent the salt water saturation temperature for the liquid phase at the starting point of the evaporation process, the convective heat transfer mechanism in the solid-liquid interphase, and insulation condition at the bottom of the sea-water container respectively.

Evaporation rate, interphase transport coefficients, and physical properties:

The Newton's law of mass transfer was used to calculate the evaporation flux from the surface of salt water into the porous-solid phase. The evaporation flux was expressed as:

$$N_w = K_Y(Y_{sat} - Y_a) \quad (8)$$

In equation (8), the mass transfer coefficient (K_Y) in the porous-solid phase was obtained using Adrie et al.¹, and Smolsky and Sergeyev² dimensionless correlations for the capillary evaporation process at laminar and the turbulent regimes respectively.

The interphase heat transfer coefficient for the motionless salt water (h_w) and air (h_a) were obtained using the Nusselt's number correlation defined by Kimura et al.³, and Pop and Cheng⁴ respectively. Sharqawy et al.⁵ polynomials were used to determine the physical properties of sea-water including the density, the specific-heat capacity, the thermal conductivity, the dynamic and kinematics viscosity, the saturation partial pressure, and the latent-heat of vaporization. The physical properties of the porous-solid material were calculated for the mixture using the porosity and the properties of the pure phases.⁶

Method of solution

Depending on the ambient and the solid phase temperature one of linear equation system comprising equations 1 and 4, or 2 and 4 should be solved simultaneously. Both ODEs and the PDE equations were solved numerically using finite difference method. For the non-homogeneous linear ODEs (equation 1 and 2), the Runge-Kutta method was used to obtain the solution. Repeated computations were performed until all calculated variables satisfied the convergence criteria.

Symbols:

α_{sw} : sea-water heat diffusivity (dimensionless).

C_{pm} : specific heat capacity of the porous-solid material (J/Kg °C).

E_{ir} : total solar irradiance received by solid materials (W/m²).

h_a : interphone heat transfer coefficient in air (W/m² °C).

h_{sw} : interphone heat transfer coefficient in sea-water (W/m² °C).

K_Y : overall mass transfer coefficient in the gas phase (Kg dry air/m².s).

K_{sw} : thermal conductivity of sea-water temperature (W/m °C).

l_s, l_{sw} : thickness and depth of the porous-solid and sea water, respectively (m).

N_w : evaporation flux of sea-water ($\text{Kg}/\text{m}^2 \cdot \text{s}$).

Pe : Peclet's Number (dimensionless).

T_a : ambient (air) temperature ($^{\circ}\text{C}$).

T_s : porous-solid material temperature ($^{\circ}\text{C}$).

T_{sw} : sea-water temperature ($^{\circ}\text{C}$).

T_{sw}^{sat} : saturation temperature of sea-water ($^{\circ}\text{C}$).

Y_a : absolute humidity of ambient air ($\text{Kg water}/\text{Kg dry air}$).

Y_{sat} : saturated absolute humidity at the gas-liquid interface ($\text{Kg water}/\text{Kg dry air}$).

z : independent variable on z axis (m).

Greek symbols:

δ : Stefan-Boltzmann constant ($5.67 \cdot 10^{-8} \text{ W}/\text{m}^2 \cdot \text{K}^4$).

ΔH_{fg} : latent heat of sea-water vaporization (J/Kg).

ϵ : radiation emissivity of the porous-solid material (dimensionless).

θ : time (S).

ρ_m : density of the porous-solid material (Kg/m^3).

ϕ : open volumetric porosity of the porous-solid material (dimensionless).

References:

1. F. G. Adrie, J. Welgraven, D. Welgraven, *Int. J. Heat Mass Transfer*, 1988, **31**, 119-127.
2. B.M. Smolsky and G.T. Sergeyeve, *Int. J. Heat Mass Transfer*, 1962, **5**, 1011-1021.
3. S. Kimura, A. Bejan, I. Pop, *J. Heat Transfer*, 1985, **107**, 819–825.
4. I. Pop, P. Cheng, *Int. J. Heat Mass Transfer*, 1983, **26**, 1574–1576.
5. M. H. Sharqawy, J. H. Lienhard, S. M. Zubair, *Desalination Water Treatment*, 2010, **16**, 354-380.
6. A. Bejan, *Convection Heat Transfer*, 2nd ed., Wiley, New York, 1995.

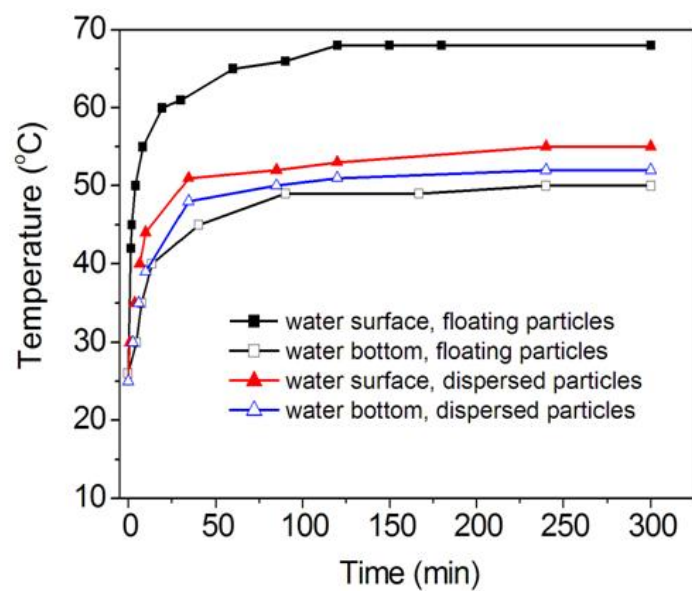


Fig. S5. The surface and bottom temperatures of 5 g of salt water added with 0.045 g of $\text{Fe}_3\text{O}_4/\text{C}$ particles change with time under the sunlight radiation.